

Deep-learning-based recognition of multi-singularity structured light

Hao Wang,^{1,2,†} Xilin Yang,^{3,†} Zeqi Liu,^{1,2} Yijie Shen,⁴ Jing Pan,^{1,2} Yuan Meng,^{1,2} Zijian Shi,^{1,2} Zhensong Wan,^{1,2} Hengkang Zhang,^{1,2} Xing Fu,^{1,2,*} Qiang Liu^{1,2,*}

¹Key Laboratory of Photonic Control Technology (Tsinghua University), Ministry of Education, Beijing 100084, China

²State Key Laboratory of Precision Measurement of Technology and Instruments, Department of Precision Instrument, Tsinghua University, Beijing 100084, China

³Electrical and Computer Engineering Department, University of California, Los Angeles, California 90095, United States

⁴Optoelectronics Research Centre, University of Southampton, Southampton SO17 1BJ, UK

Abstract: Structured light with customized complex topological pattern inspires diverse classical and quantum investigations underpinned by accurate detection techniques. However, the current detection schemes are limited to vortex beam with simple phase singularity. The precise recognition of general structured light with multiple singularities remains elusive. Here, we report a deep learning (DL) framework that can unveil multi-singularity phase structures in an end-to-end manner after feeding only two intensity patterns upon beam propagation captured via a camera, thus unleashing intuitive information of twisted photons. The DL toolbox can also acquire phases of Laguerre-Gaussian (LG) modes with single singularity and other general phase objects likewise. Leveraging this DL platform, a phase-based optical secret sharing (OSS) protocol is proposed, which is based on a more general class of multi-singularity modes than conventional LG beams. The OSS protocol features strong security, wealthy state space and convenient intensity-based measurements. This study opens new avenues for vortex beam communications, laser mode analysis, microscopy, Bose-Einstein condensates characterization, etc.

Keywords: structured light; vortex beams; orbital angular momentum; deep learning; optical secret key sharing

1 Introduction

In addition to linear momentum, photons can carry angular momentum divided into two forms, spin and orbital [1,2]. The spin angular momentum usually refers to light's polarization [3], and the orbital angular momenta (OAM) arises if the wavefront is helically shaped with a phase singularity on axis [4]. The typical unit of the helical phase is the azimuthal dependence $e^{i\ell\varphi}$, where ℓ reveals topological charge (TC) and φ is the azimuthal angle [5]. In contrast to conventional vortex beams with single singularity, e.g. Laguerre-Gaussian (LG) and Bessel modes, recent advances highlight the general structured light with distributions of multiple singularities, such as singularity array [6,7], vortex lattices [8], and SU(2) vortex geometric modes [9-11]. Vortex beams have triggered intense research over the past three decades [12] for their potentials in both classical (optical tweezers [13,14], holographic encryption [15], communications [16], measurements [17,18], nonlinear effects [19,20]) and quantum applications (quantum secret sharing [21], quantum switches [22], quantum information processing [23], quantum states tomography [24]). For most of these pertinent application scenarios using optical vortices, accurate detection of OAM is a basic premise, which may resort to interference [25], diffraction [26], log-polar transformation [27], spiral

transformation [28], multiplane light conversion [29], and deep learning algorithms [30], to name a few.

However, the current detection methods mainly work for single-singularity vortices. The precise measurement of more complex multi-singularity counterparts still remains a demanding task. This task requires detecting all vortices first and quantifying each vortex then. On the other hand, all the topological information of optical vortices is stored in phase whereupon a relevant issue arises: can we decode the phase directly? Indeed, phase recovery in the presence of singularities is a long-standing bugbear [31,32]. Researchers have invoked transport of intensity equation (TIE) [33], Gerchberg-Saxton based algorithm [34], wavefront modulation [35,36], diffractive imaging [37-39], or interferometer [40,41], to retrieve the phases of vortex beams. However, these profound endeavors still suffer from requiring multiple high-precision ($\sim\mu\text{m}$) axial intensity measurements and rigorous boundary conditions, or non-intuitive iterative algorithms, or much *a priori* knowledge, or being vulnerable to experimental noises. Most importantly, many methods are feasible for simple vortices only and the recovered performances were unfulfilling.

In this work, we propose a deep learning framework, which is dubbed "VortexNet", to overcome these hurdles. It's mention-worthy that recent years have witnessed transformative advances of deep neural networks in

analyzing vortex light, spanning from scalar [30,42-48] to vectorial ones [49]. Most previous achievements regard single-singularity OAM recognition as a classification or a regression task. The outputs of their networks are only simple numbers, which relate to the exact TCs. However, we here handle it as a generative problem whereby VortexNet yields complex phases containing dozens of singularities in an end-to-end manner, thus unleashing rich and intuitive physics information to comprehend twisted photons. Here we demonstrate the phase reconstruction approach onto a set of multi-singularity SU(2) vortex modes, which accommodate conventional LG vortex modes as simple members and characterize high-dimensional topological properties [50]. Benefitting from the satisfactory performance of VortexNet, a phase-based optical secret sharing (OSS) protocol is demonstrated as an exemplary application. VortexNet can acquire phases of SU(2) beams with mode accuracy up to 93.6% from only two measurements of intensity. It also works for LG modes even with large TCs and degenerate intensities as well as other general phase objects. Therefore, it is a universal and practical tool for many classical and quantum information processing systems.

2 Methods

As a typical example of complex vortex beams with multiple singularities, SU(2) mode can be excited in a special resonator [51] and it can be launched by coherently superposing a set of LG modes,

$$\psi_{Q,n_0,M}(x,y,z;\phi) = S(\psi_{p,\ell}^{LG}), \quad (1)$$

where $\psi_{p,\ell}^{LG}$ represents LG mode with radial index p and angular index ℓ . The function $S(*)$ is defined to describe SU(2) superposition rule briefly, integer Q refers to how many folds in the rotational symmetry, n_0 decides the TC of axial vortex, M reveals its localized OAM of off-axis singularities and $\phi \in (0, 2\pi)$ determines initial phase. Each SU(2) vortex mode corresponds to a pair of parameters (Q, n_0, M) unravelling the topological information. By utilizing the multiple parameters of SU(2) modes, researchers successfully realized the classical analogy of high-dimensional quantum Greenberger-Horne-Zeilinger states recently [50]. Figure 1 illustrates the difference between circular shaped LG mode $(p, \ell) = (0, 8)$ whose intensity always remains in circular symmetry, and SU(2) mode $(Q, n_0, M) = (4, 8, 9)$ which is favored with large OAM, multiple singularities, helical star-shaped pattern and spiral propagation trajectory (See Supplemental Material I for more details of SU(2) modes).

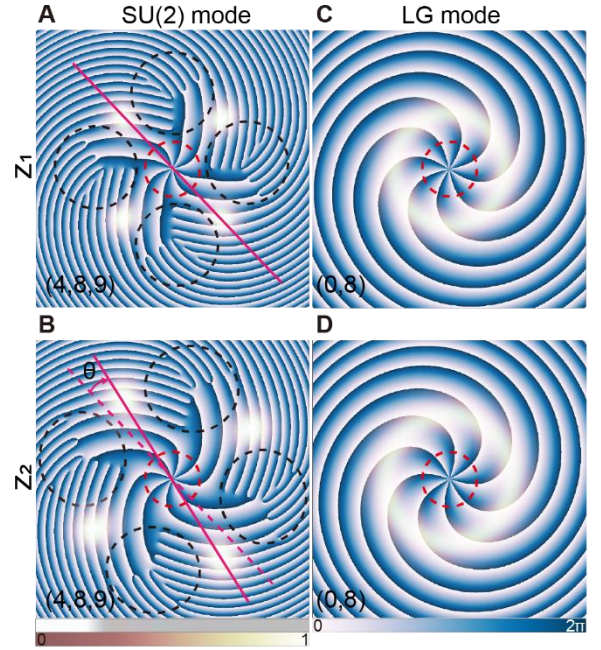


Figure 1: Comparison of SU(2) vortex mode (A)-(B) and LG mode (C)-(D) at two axial positions. Other than the single singularity of LG mode induced by central OAM as indicated by red circles, SU(2) mode characterizes more singularities shown by black circles. Besides, as SU(2) mode propagates from z_1 (a) to z_2 (b), its intensity undergoes an azimuthal shift θ while that of LG mode remains circularly symmetric. Note the intensity layers are set with opacity.

Inspired by TIE [32,52], a prevailing benchmark model in phase retrieval assignments, wherein the phase at the target plane can be unwrapped given the target-plane intensity and intensity differential, we construct VortexNet to calculate phases based on *two* intensity patterns I_1 and I_2 as elucidated in Figure 1: one is that of target plane,

$$I_1 = |\psi_{Q,n_0,M}(x,y,z_r;\phi)|^2, \quad (2)$$

where z_r is the Rayleigh distance. The other is the intensity pattern of the defocused plane,

$$I_2 = |\psi_{Q,n_0,M}(x,y,z_r + \Delta z;\phi)|^2, \quad (3)$$

where Δz is the diffraction distance after the target plane. In the experiment, the defocused light can be characterized by

$$\psi_{Q,n_0,M}(x,y,z_r + \Delta z;\phi) = \frac{\exp(ik\Delta z)}{i\lambda\Delta z} \exp\left[i\frac{k(x^2 + y^2)}{2\Delta z}\right] \mathcal{F}\left\{\psi_{Q,n_0,M}(x_0,y_0,z_r;\phi) \exp\left[i\frac{k(x_0^2 + y_0^2)}{2\Delta z}\right]\right\}_{f_x=\frac{x}{\lambda\Delta z}, f_y=\frac{y}{\lambda\Delta z}}, \quad (4)$$

where $k = 2\pi/\lambda$ is the wavenumber, $\mathcal{F}(*)$ denotes the spatial Fourier transformation. As a notable example, we plot these two experimental patterns of mode $(Q, n_0, M) = (5, 6, 7)$ in the inset of Figure 2. With visible I_1 and I_2 as inputs at hand, VortexNet is expected to reconstruct the

invisible phase,

$$P_{Q,n_0,M}(x,y,z_r;\phi) = \arg[\psi_{Q,n_0,M}(x,y,z_r;\phi)], \quad (5)$$

where $\arg(*)$ returns the argument of a complex variable.

To train the VortexNet, massive data samples are necessary. Rather than utilizing a laser cavity, which is challenging for efficient on-demand modes generation, we collect datasets via spatial light modulator (SLM) as illustrated in Figure 2. More specifically, a 532 nm laser (CNI Laser, MGL-III-532) is employed as the source of Gaussian beam. After being expanded eightfold, it undergoes modulation of the SLM (Hamamatsu, X13138-04, resolution of 1280×1024 , pixel size of $12.5 \mu\text{m}$). The $SU(2)$ state $\psi_{Q,n_0,M}(x,y,z_r;\phi)$ is encoded into the computer-generated-holographic mask through complex amplitude modulation technique [53,54]. Two lenses L1 (150 mm) and L2 (75 mm) constitute a 4-f system, through which the conjugate image of target vortex mode is recorded by the CMOS camera (AVT Mako G-131B, resolution of 1280×1024 , pixel size of $5.3 \mu\text{m}$), which completes our first measurement. Then the CMOS is moved backward for 10.00 mm through a one-dimensional translation stage (GCM-830303M, resolution of 0.01 mm), leading to a weak diffraction of the $SU(2)$ mode, the intensity of which is recorded as the second measurement.

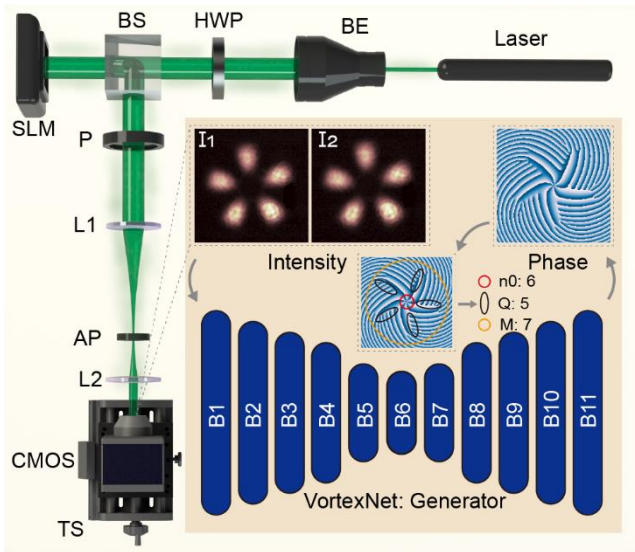


Figure 2: Schematic of experimental layout for the $SU(2)$ mode creation and vortex phase acquisition. BE: beam expander; HWP: half-wave plate, which aligns the source to be p-polarized; BS: beam splitter, which assures the optical structure is rectangular; SLM: spatial light modulator; P: polarizer, which adjusts the light intensity; L1, L2: lens; AP: aperture, which filters out the first diffraction order; CMOS: camera; TS: translation stage, which moves the CMOS in z direction. After recording two intensity patterns with a longitudinal interval of 10.00 mm, the generator of VortexNet reconstructs the phase and then the value of the parameters

(Q, n_0, M) can be decoded accordingly. B: block, configurable unit of the generator part of VortexNet.

VortexNet is inherently an adapted conditional generative adversarial network (cGAN) (See Supplemental Material III for network details), containing a generator and a discriminator [55,56]. GANs are an instrumental category of deep neural networks with ever-improving results that can extract the hierarchical features of input data and enhance the prediction accuracy [57]. In this case, the generator outputs a “fake phase” and this output along with labelled phase (true phase) are both fed into the discriminator. The discriminator strives to evaluate whether the input is real or fake. The two networks are trained jointly and they reach the “Nash equilibrium” when the training ends [58]. At this moment, the discriminator struggles to distinguish true or false and the generator returns a convincing phase.

3 Results

The network is first trained using an experimental dataset with mode parameters $Q \in \{3, 4, 5, 6\}$, $n_0 \in \{1, 2, \dots, 10\}$ and $M \in \{1, 2, \dots, 10\}$ (See Supplemental Material II.A for dataset acquisition details). For each set of parameters (Q, n_0, M) , the initial phase ranges from 0 to 1.96π with an incremental value of 0.04π . There are overall 400 different states and 20000 pairs of intensity images within the experimental dataset. Among them, we select 86% for training, 10% for validating and 4% for testing the VortexNet. Some blind test results are shown in Figure 3(A)-(D), showing excellent agreement between the ground truth and network output (See more in Supplemental Material II.B). Once the generator performs inference of the phase, one can decode the carried information of $SU(2)$ mode. Based on three phase read-out rules defined in Supplemental Material I, the recognition accuracies of parameters Q , n_0 and M are summarized in the confusion matrixes of Figure 4. The *accuracy* refers to the proportion of correctly classified modes and is calculated by comparing the reconstructed phase with respect to its corresponding ground truth. Accuracies of both Q and M reach 100% while n_0 achieves 93.6%. Hence the overall mode accuracy of 93.6% is already obtained. To further evaluate the quality of generated phase structures quantitatively, we calculate the peak-signal-to-noise (PSNR), structural similarity index (SSIM) and image correlation coefficient (CC) metrics. The average values of them are 14.89 dB, 0.75 and 0.76 respectively (See Supplemental Material II.B for details). These values are not that prominent because of nonideal experimental conditions like power fluctuation of laser source, lens glare, and CMOS

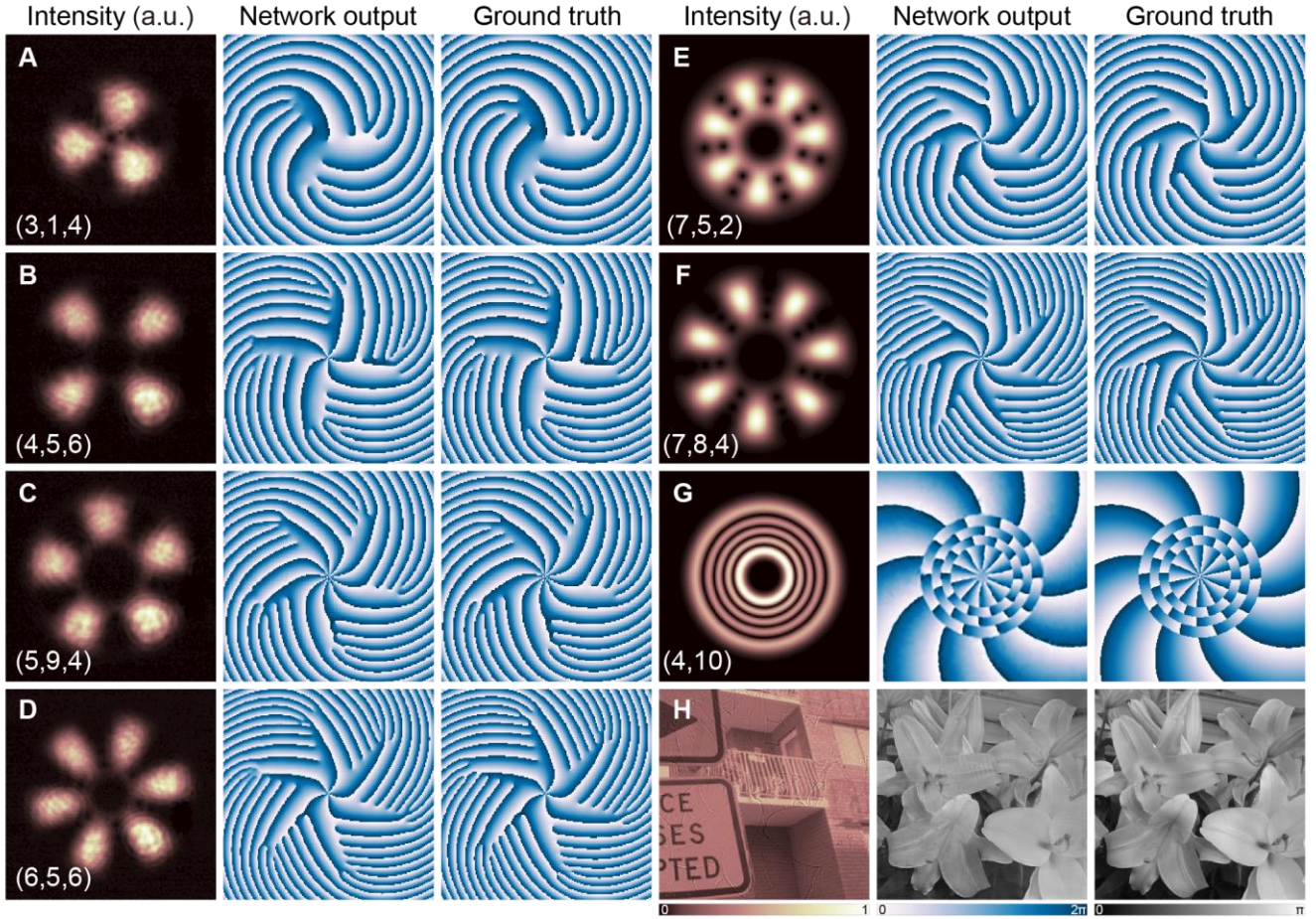


Figure 3: Inference results of VortexNet on experimental test set (A)-(D), modes out of training, validation and test set (E)-(F), LG modes (G) and general phase objects (H). First and fourth column: normalized intensity; Second and fifth column: VortexNet output; Third and sixth column: phase ground truth. More results are available in Supplementary Materials B.

noise. These imperfections are incorporated into the training process to beset the metrics of reconstructed phase. However, thanks to the read-out rule, some local flaws may degrade three metrics, they don't mislead us to identify the mode parameters and the mode accuracy of 93.6% is still acceptable. We note that with an improved system, the results can be enhanced. To validate this claim, we retrained a VortexNet based on exclusively simulated intensities and the mean PSNR, SSIM and CC are improved to be 16.46dB, 0.84 and 0.85. Remarkably, the recognition accuracy of (Q, n_0, M) reaches 100%.

Later, to confirm VortexNet is learning to transform extracted features into phase structures rather than memorizing all the modes and overfitting the training set, we establish the second test set containing 64 states where $Q = 7, n_0 \in \{1, 2, \dots, 8\}, M \in \{1, 2, \dots, 8\}$, which separate from training, validation and the first test set. We let the trained model based on digitally generated dataset to infer. Two results are depicted in Figure 3(E)-(F) with the overall accuracy reaching 93.75% and the average PSNR, SSIM, CC being 12.00 dB, 0.57, and 0.58.

In order to analyze the physics-informed training phase of VortexNet, i.e. why two intensity measurements are inevitable, we naturally train a model with only I_1 as input. It's a strongly ill-posed inverse problem to retrieve $P_{Q, n_0, M}(x, y, z_r; \phi)$ and indeed the poor blind testing results in Supplemental Material II.C bear this out. Interestingly, we train another VortexNet akin to TIE, i.e. we now input I_1 and a differential approximated as $I_{diff} = (I_1 - I_2)/\Delta z$. The convergence time and mode accuracy result are similar to that of I_1 and I_2 as input. It's quite reasonable because a linear operation does not diminish the amount of information and is easily learnable for deep neural networks.

In addition, we realize that this computational network not only can be applied for multi-singularity vortex modes, but also more universal phase reconstruction missions. Part of the LG modes results as well as other general phase images based on simulated datasets are illustrated in Figure 3(G)-(H) (See more in Supplemental Material II.D). It's notable that VortexNet trained with proper dataset can effectively solve the intensity degenerate problem that previous endeavors encountered [30,43], where the intensities of $\psi_{p,\ell}^{LG}$ and $\psi_{p,-\ell}^{LG}$ are identical to make

previous network unable to distinguish.

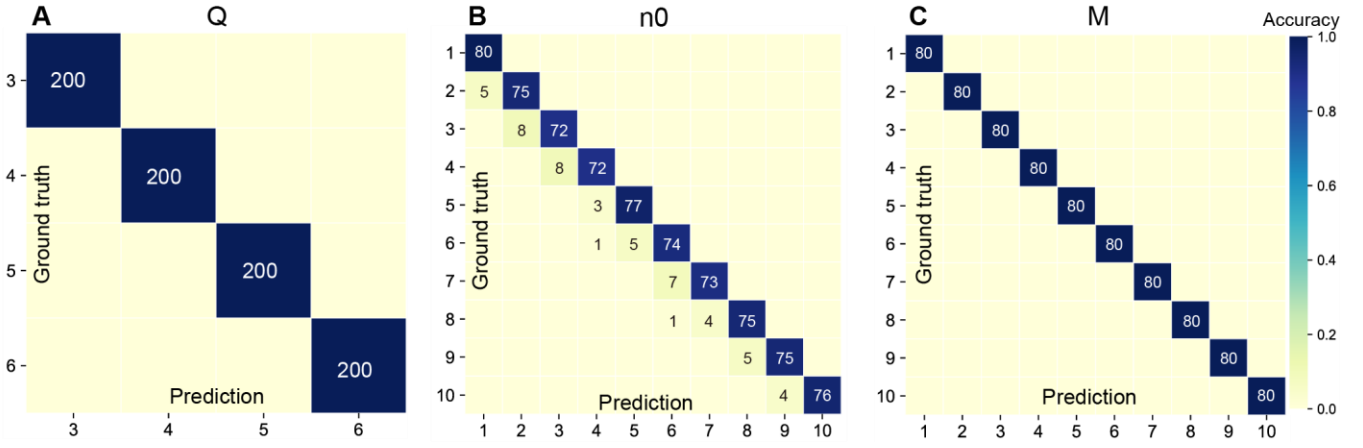


Figure 4: The confusion matrixes of experimental testing results, indicating the number of correctly (diagonal) and incorrectly (off-diagonal) predicted mode parameters (A) Q , (B) n_0 and (C) M . Note the color of every box reflects the normalized accuracy.

As we discussed before, VortexNet can directly deliver phases of SU(2) modes through indiscernible intensities hence it opens new pathways for utilizing high-dimensional topological properties in information dissemination. As data security becomes increasingly crucial, optical-based secret sharing thrives due to its abundant degrees of freedom, broad bandwidth and susceptibility to eavesdropping [59,60]. We, therefore, devise a phase-based OSS protocol enabled by VortexNet as depicted in Figure 5.

complicate the message, we allot a bundle of SU(2) light to every player. Based on the experimental scheme in Figure 2, we implement the allocation operation through four holograms and in fact this can also be implemented technically via one hologram that customizes four diffraction orders of further [61]. Every player takes two shots of in incoming light coming SU(2) beam as his/her share of the secret. To decrypt the key, firstly all shareholders need to interpret two pieces of intensities through VortexNet, which is held in the hands of “the president”, who will then honestly take out their shares based on retrieved phases and adopt bitwise XOR operation. The high security stems from exotic and noninterpretable SU(2) intensity patterns, wealthy state space and additional layer endowed by VortexNet.

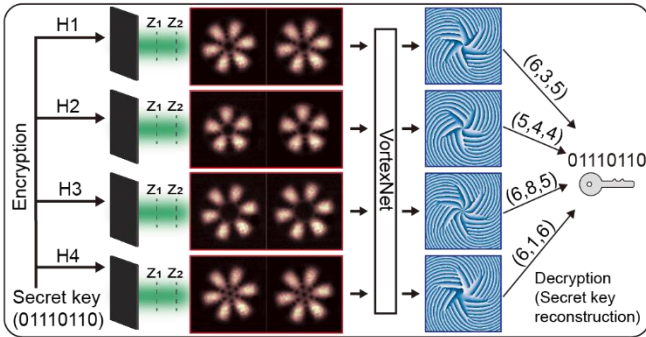


Figure 5: The phase-based OSS workflow. The secret key is encrypted into holograms (H1, H2, H3 and H4) that modulate the incoming light into distinct SU(2) modes. Each shareholder catches two intensities of SU(2) mode at position z_1 and z_2 . The decryption must involve honest collaboration and VortexNet to calculate the phases.

First we allocate every mode (Q, n_0, M) to an 8-bit binary number (See Supplemental Material IV for detailed rules). Suppose the secret S is encoded as an 8-bit binary number (01110110 in this case) and in a traditional secret sharing scheme, the distributor will give three of four shareholder each a random 8-bit number (N_1, N_2 , and N_3). The last player has to get the result of $S \oplus N_1 \oplus N_2 \oplus N_3$, where \oplus denotes bitwise exclusive or (XOR). Instead, to

4 Discussions and conclusions

The general significance of VortexNet covers several aspects: it is envisaged to recover phases of other multi-singularity beams such as vortex lattice [62] as well as diverse categories of structured light—LG beam, Airy beam and Bessel beam, to name a few—it liberates us by encoding/decoding *phase* information from only caring about intensity utilizations of shaped beams. The network structure can also be cascaded with another GAN which accommodates VortexNet’s phase as input and gives mode parameters directly [63]. This way the detection is reduced to be like Refs. [30,49]. In experiments, the intensity interval is fixed to be 10.00 mm, which doesn’t pose rigorous conditions for implementation. And the network is robust against small misalignment. The adverse atmosphere turbulence on structured light may be mitigated by an improved VortexNet without recourse to a probe beam [64] in future research. In addition, VortexNet can also be

enforced on complex amplitude reconstruction assignments, which can aid in digital holographic imaging [65]. Besides, the OSS is scalable both in terms of SU(2) modes number and secret-splitting rule. The first point concerns that as the neural networks nowadays progress towards bigger model architecture, bigger dataset and stronger computation power, one can scale up the SU(2) modes and construct a benchmark dataset/library for more sophisticated encryption. Secondly, the proposed OSS can be readily extended to $(t, n) - threshold$ scheme where t or more of n players can decipher the key, and also grafted onto classical Shamir's scheme, the Chinese remainder theorem-based scheme, etc. Furthermore, one can adopt the affluent SU(2) states to transmit information in a mode-multiplexing or shift-keying manner [66,67]. Notably, when a frequency-degenerate resonator emits SU(2) modes in the lab, one has to blindly select (Q, n_0, M) in simulation to find the most similar one to characterize the emission mode due to non-interpretable intensity pattern before. Now VortexNet raises a hand to do the mode analysis job, which greatly facilitates the development of structured beam laser [68]. Last but not the least, the VortexNet-based techniques may also find further applications on electronic, X-ray as well as acoustics systems.

To conclude, we demonstrate a new approach to tackling structured beams enabled by deep learning, in particular phases with single/multiple singularities. The topological properties are revealed directly, accurately and robustly by using only two convenient intensity-based measurements as inputs, even in the presence of inherent noises and instabilities. Empowered by SU(2) vortex modes with high-dimensional quantum analogy properties and great state space, numerous schemes employing them as information carriers are feasible now and we demonstrate a novel OSS protocol as an instance. This DL-assisted platform may promise relevant implications in OAM communications [48], laser mode analysis [68], microscopy [69], Bose-Einstein condensates characterization [70], etc.

We acknowledge Jia Guo, Lin Zhang, Yan Wang and Jiading Tian. This work is supported by the National Natural Science Foundation of China (61875100) and National Natural Science Foundation of China (61975087).

*Corresponding author.

qiangliu@tsinghua.edu.cn

fluxing@tsinghua.edu.cn

†H.W. and X.Y. contributed equally to this work.

References

- [1] L. Allen, M. W. Beijersbergen, R. J. C. Spreeuw, and J. P. Woerdman, Orbital angular momentum of light and the transformation of Laguerre-Gaussian laser modes, *Phys. Rev. A* **45**, 8185 (1992).
- [2] W. J. Firth and D. V. Skryabin, Optical Solitons Carrying Orbital Angular Momentum, *Phys. Rev. Lett.* **79**, 2450 (1997).
- [3] D. L. P. Vitullo, C. C. Leary, P. Gregg, R. A. Smith, D. V. Reddy, S. Ramachandran, and M. G. Raymer, Observation of Interaction of Spin and Intrinsic Orbital Angular Momentum of Light, *Phys. Rev. Lett.* **118**, 083601 (2017).
- [4] A. T. O'Neil, I. MacVicar, L. Allen, and M. J. Padgett, Intrinsic and Extrinsic Nature of the Orbital Angular Momentum of a Light Beam, *Phys. Rev. Lett.* **88**, 053601 (2002).
- [5] G. Molina-Terriza, J. P. Torres, and L. Torner, Twisted photons, *Nat. Phys.* **3**, 305 (2007).
- [6] E. Brasselet, Tunable Optical Vortex Arrays from a Single Nematic Topological Defect, *Phys. Rev. Lett.* **108**, 087801 (2012).
- [7] X. Qiu, F. Li, H. Liu, X. Chen, and L. Chen, Optical vortex copier and regenerator in the Fourier domain, *Photonics Res.* **6**, 641 (2018).
- [8] R. Barboza, U. Bortolozzo, G. Assanto, E. Vidal-Henriquez, M. G. Clerc, and S. Residori, Harnessing Optical Vortex Lattices in Nematic Liquid Crystals, *Phys. Rev. Lett.* **111**, 093902 (2013).
- [9] Y. F. Chen, T. H. Lu, and K. F. Huang, Observation of Spatially Coherent Polarization Vector Fields and Visualization of Vector Singularities, *Phys. Rev. Lett.* **96**, 033901 (2006).
- [10] Y. Shen, Z. Wang, X. Fu, D. Naidoo, and A. Forbes, SU(2) Poincare sphere: A generalized representation for multidimensional structured light, *Phys. Rev. A* **102**, 031501 (2020).
- [11] Y. Shen, X. Yang, D. Naidoo, X. Fu, and A. Forbes, Structured ray-wave vector vortex beams in multiple degrees of freedom from a laser, *Optica* **7**, 820 (2020).
- [12] Y. Shen, X. Wang, Z. Xie, C. Min, X. Fu, Q. Liu, M. Gong, and X. Yuan, Optical vortices 30 years on: OAM manipulation from topological charge to multiple singularities, *Light Sci. Appl.* **8**, 90 (2019).
- [13] A. Alexandrescu, D. Cojoc, and E. D. Fabrizio, Mechanism of Angular Momentum Exchange between Molecules and Laguerre-Gaussian Beams, *Phys. Rev. Lett.* **96**, 243001 (2006).
- [14] M. Padgett and R. Bowman, Tweezers with a twist, *Nat. Photonics* **5**, 343 (2011).
- [15] X. Fang, H. Ren, and M. Gu, Orbital angular momentum holography for high-security encryption, *Nat. Photonics* **14**,

102 (2020).

- [16] Z. Zhu, M. Janasik, A. Fyffe, D. Hay, Y. Zhou, B. Kantor, T. Winder, R. W. Boyd, G. Leuchs, and Z. Shi, Compensation-free high-dimensional free-space optical communication using turbulence-resilient vector beams, *Nat. Commun.* **12**, 1666 (2021).
- [17] J. Ni, S. Liu, D. Wu, Z. Lao, Z. Wang, K. Huang, S. Ji, J. Li, Z. Huang, Q. Xiong *et al.*, Gigantic vortical differential scattering as a monochromatic probe for multiscale chiral structures, *Proc. Natl. Acad. Sci. U.S.A.* **118**, e2020055118 (2021).
- [18] S. Barreiro, J. W. R. Tabosa, H. Failache, and A. Lezama, Spectroscopic Observation of the Rotational Doppler Effect, *Phys. Rev. Lett.* **97**, 113601 (2006).
- [19] Y. Chen, R. Ni, Y. Wu, L. Du, X. Hu, D. Wei, Y. Zhang, and S. Zhu, Phase-Matching Controlled Orbital Angular Momentum Conversion in Periodically Poled Crystals, *Phys. Rev. Lett.* **125**, 143901 (2020).
- [20] Y. Tang, K. Li, X. Zhang, J. Deng, G. Li, and E. Brasselet, Harmonic spin-orbit angular momentum cascade in nonlinear optical crystals, *Nat. Photonics* **14**, 658 (2020).
- [21] J. Pinnell, I. Nape, M. de Oliveira, N. TabeBordbar, and A. Forbes, Experimental Demonstration of 11-Dimensional 10-Party Quantum Secret Sharing, *Laser Photonics Rev.* **14**, 2000012 (2020).
- [22] K. Goswami, C. Giarmatzi, M. Kewming, F. Costa, C. Branciard, J. Romero, and A. G. White, Indefinite Causal Order in a Quantum Switch, *Phys. Rev. Lett.* **121**, 090503 (2018).
- [23] M. Erhard, R. Fickler, M. Krenn, and A. Zeilinger, Twisted photons: new quantum perspectives in high dimensions, *Light Sci. Appl.* **7**, 17146 (2018).
- [24] E. Toninelli, B. Ndagano, A. Vallés, B. Sephton, I. Nape, A. Ambrosio, F. Capasso, M. J. Padgett, and A. Forbes, Concepts in quantum state tomography and classical implementation with intense light: a tutorial, *Adv. Opt. Photonics* **11**, 67 (2019).
- [25] A. Ariyawansa, E. J. Figueroa, and T. G. Brown, Amplitude and phase sorting of orbital angular momentum states at low light levels, *Optica* **8**, 147 (2021).
- [26] J. M. Hickmann, E. J. S. Fonseca, W. C. Soares, and S. Chávez-Cerda, Unveiling a Truncated Optical Lattice Associated with a Triangular Aperture Using Light's Orbital Angular Momentum, *Phys. Rev. Lett.* **105**, 053904 (2010).
- [27] G. C. G. Berkhout, M. P. J. Lavery, J. Courtial, M. W. Beijersbergen, and M. J. Padgett, Efficient Sorting of Orbital Angular Momentum States of Light, *Phys. Rev. Lett.* **105**, 153601 (2010).
- [28] Y. Wen, I. Chremmos, Y. Chen, J. Zhu, Y. Zhang, and S. Yu, Spiral Transformation for High-Resolution and Efficient Sorting of Optical Vortex Modes, *Phys. Rev. Lett.* **120**, 193904 (2018).
- [29] N. K. Fontaine, R. Ryf, H. Chen, D. T. Neilson, K. Kim, and J. Carpenter, Laguerre-Gaussian mode sorter, *Nat. Commun.* **10**, 1865 (2019).
- [30] Z. Liu, S. Yan, H. Liu, and X. Chen, Superhigh-Resolution Recognition of Optical Vortex Modes Assisted by a Deep-Learning Method, *Phys. Rev. Lett.* **123**, 183902 (2019).
- [31] L. J. Allen, H. M. L. Faulkner, K. A. Nugent, M. P. Oxley, and D. Paganin, Phase retrieval from images in the presence of first-order vortices, *Phys. Rev. E* **63**, 037602 (2001).
- [32] C. Zuo, J. Li, J. Sun, Y. Fan, J. Zhang, L. Lu, R. Zhang, B. Wang, L. Huang, and Q. Chen, Transport of intensity equation: a tutorial, *Opt. Lasers Eng.* **135**, 106187 (2020).
- [33] A. Lubk, G. Guzzinati, F. Börrnert, and J. Verbeeck, Transport of Intensity Phase Retrieval of Arbitrary Wave Fields Including Vortices, *Phys. Rev. Lett.* **111**, 173902 (2013).
- [34] P. A. A. Yasir and J. S. Ivan, Estimation of phases with dislocations in paraxial wave fields from intensity measurements, *Phys. Rev. A* **97**, 023817 (2018).
- [35] F. Zhang, G. Pedrini, and W. Osten, Phase retrieval of arbitrary complex-valued fields through aperture-plane modulation, *Phys. Rev. A* **75**, 043805 (2007).
- [36] L. Zhao, K. Wang, and J. Bai, Large-scale phase retrieval method for wavefront reconstruction with multi-stage random phase modulation, *Opt. Commun.* **498**, 127115 (2021).
- [37] A. V. Martin and L. J. Allen, Phase imaging from a diffraction pattern in the presence of vortices, *Opt. Commun.* **277**, 288 (2007).
- [38] J. Vila-Comamala, A. Sakdinawat, and M. Guizar-Sicairos, Characterization of x-ray phase vortices by ptychographic coherent diffractive imaging, *Opt. Lett.* **39**, 5281 (2014).
- [39] C. A. Henderson, G. J. Williams, A. G. Peele, H. M. Quiney, and K. A. Nugent, Astigmatic phase retrieval: an experimental demonstration, *Opt. Express* **17**, 11905 (2009).
- [40] J. Guo, S. Zheng, K. Zhou, and G. Feng, Measurement of real phase distribution of a vortex beam propagating in free space based on an improved heterodyne interferometer, *Appl. Phys. Lett.* **119**, 023504 (2021).
- [41] F. Venturi, M. Campanini, G. C. Gazzadi, R. Balboni, S. Frabboni, R. W. Boyd, R. E. Dunin-Borkowski, E. Karimi, and V. Grillo, Phase retrieval of an electron vortex beam using diffraction holography, *Appl. Phys. Lett.* **111**, 223101 (2017).
- [42] S. Lohani and R. T. Glasser, Turbulence correction with artificial neural networks, *Opt. Lett.* **43**, 2611 (2018).
- [43] Z. Mao, H. Yu, M. Xia, S. Pan, D. Wu, Y. Yin, Y. Xia, and J. Yin, Broad Bandwidth and Highly Efficient Recognition of Optical Vortex Modes Achieved by the Neural-Network Approach, *Phys. Rev. Applied* **13**, 034063 (2020).

- [44] P. L. Neary, J. M. Nichols, A. T. Watnik, K. P. Judd, G. K. Rohde, J. R. Lindle, and N. S. Flann, Transport-based pattern recognition versus deep neural networks in underwater OAM communications, *J. Opt. Soc. Am. A* **38**, 954 (2021).
- [45] X. Wang, Y. Qian, J. Zhang, G. Ma, S. Zhao, R. Liu, H. Li, P. Zhang, H. Gao, F. Huang *et al.*, Learning to recognize misaligned hyperfine orbital angular momentum modes, *Photonics Res.* **9**, B81 (2021).
- [46] B. P. da Silva, B. A. D. Marques, R. B. Rodrigues, P. H. S. Ribeiro, and A. Z. Khoury, Machine-learning recognition of light orbital-angular-momentum superpositions, *Phys. Rev. A* **103**, 063704 (2021).
- [47] X. Wang, T. Wu, C. Dong, H. Zhu, Z. Zhu, and S. Zhao, Integrating deep learning to achieve phase compensation for free-space orbital-angular-momentum-encoded quantum key distribution under atmospheric turbulence, *Photonics Res.* **9**, B9 (2021).
- [48] M. Krenn, J. Handsteiner, M. Fink, R. Fickler, R. Ursin, M. Malik, and A. Zeilinger, Twisted light transmission over 143 km, *Proc. Natl. Acad. Sci. U.S.A.* **113**, 13648 (2016).
- [49] T. Giordani, A. Suprano, E. Polino, F. Acanfora, L. Innocenti, A. Ferraro, M. Paternostro, N. Spagnolo, and F. Sciarrino, Machine Learning-Based Classification of Vector Vortex Beams, *Phys. Rev. Lett.* **124**, 160401 (2020).
- [50] Y. Shen, I. Nape, X. Yang, X. Fu, M. Gong, D. Naidoo, and A. Forbes, Creation and control of high-dimensional multipartite classically entangled light, *Light Sci. Appl.* **10**, 50 (2021).
- [51] Y. C. Lin, T. H. Lu, K. F. Huang, and Y. F. Chen, Model of commensurate harmonic oscillators with SU(2) coupling interactions: Analogous observation in laser transverse modes, *Phys. Rev. E* **85**, 046217 (2012).
- [52] J. A. Schmalz, T. E. Gureyev, D. M. Paganin, and K. M. Pavlov, Phase retrieval using radiation and matter-wave fields: Validity of Teague's method for solution of the transport-of-intensity equation, *Phys. Rev. A* **84**, 023808 (2011).
- [53] Z. Wan, Z. Wang, X. Yang, Y. Shen, and X. Fu, Digitally tailoring arbitrary structured light of generalized ray-wave duality, *Opt. Express* **28**, 31043 (2020).
- [54] V. Arrizón, U. Ruiz, R. Carrada, and L. A. González, Pixelated phase computer holograms for the accurate encoding of scalar complex fields, *J. Opt. Soc. Am. A* **24**, 3500 (2007).
- [55] Ian, J. Pouget-Abadie, M. Mirza, B. Xu, D. Warde-Farley, S. Ozair, A. Courville, and Y. Bengio, Generative Adversarial Networks, arXiv:1406.2661 (2014).
- [56] M. Mirza and S. Osindero, Conditional Generative Adversarial Nets, arXiv:1411.1784 (2014).
- [57] Y. Bengio, Y. Lecun, and G. Hinton, Deep learning for AI, *Communications of the ACM* **64**, 58 (2021).
- [58] J. Jiang, M. Chen, and J. A. Fan, Deep neural networks for the evaluation and design of photonic devices, *Nature Reviews Materials* **6**, 679 (2021).
- [59] P. Zheng, Q. Dai, Z. Li, Z. Ye, J. Xiong, H.-C. Liu, G. Zheng, and S. Zhang, Metasurface-based key for computational imaging encryption, *Science Advances* **7**, eabg0363 (2021).
- [60] P. Georgi, Q. Wei, B. Sain, C. Schlickriede, Y. Wang, L. Huang, and T. Zentgraf, Optical secret sharing with cascaded metasurface holography, *Science Advances* **7**, eabf9718 (2021).
- [61] H. Wang, S. Fu, and C. Gao, Tailoring a complex perfect optical vortex array with multiple selective degrees of freedom, *Opt. Express* **29**, 10811 (2021).
- [62] L. Zhu, M. Tang, H. Li, Y. Tai, and X. Li, Optical vortex lattice: an exploitation of orbital angular momentum, *Nanophotonics* **10**, 2487 (2021).
- [63] X. Yang, L. Huang, Y. Luo, Y. Wu, H. Wang, Y. Rivenson, and A. Ozcan, Deep-Learning-Based Virtual Refocusing of Images Using an Engineered Point-Spread Function, *ACS Photonics* **8**, 2174 (2021).
- [64] S. Fu, T. Wang, S. Zhang, Z. Zhang, Y. Zhai, and C. Gao, Non-probe compensation of optical vortices carrying orbital angular momentum, *Photonics Res.* **5**, 251 (2017).
- [65] Y. Baek and Y. Park, Intensity-based holographic imaging via space-domain Kramers–Kronig relations, *Nat. Photonics* **15**, 354 (2021).
- [66] J. Wang, J.-Y. Yang, I. M. Fazal, N. Ahmed, Y. Yan, H. Huang, Y. Ren, Y. Yue, S. Dolinar, M. Tur *et al.*, Terabit free-space data transmission employing orbital angular momentum multiplexing, *Nat. Photonics* **6**, 488 (2012).
- [67] S. Fu, Y. Zhai, H. Zhou, J. Zhang, T. Wang, X. Liu, and C. Gao, Experimental demonstration of free-space multi-state orbital angular momentum shift keying, *Opt. Express* **27**, 33111 (2019).
- [68] A. Forbes, Structured Light from Lasers, *Laser Photonics Rev.* **13**, 1900140 (2019).
- [69] B. J. McMorran, A. Agrawal, I. M. Anderson, A. A. Herzing, H. J. Lezec, J. J. McClelland, and J. Unguris, Electron Vortex Beams with High Quanta of Orbital Angular Momentum, *Science* **331**, 192 (2011).
- [70] M.-S. Kwon, B. Y. Oh, S.-H. Gong, J.-H. Kim, H. K. Kang, S. Kang, J. D. Song, H. Choi, and Y.-H. Cho, Direct Transfer of Light's Orbital Angular Momentum onto a Nonresonantly Excited Polariton Superfluid, *Phys. Rev. Lett.* **122**, 045302 (2019).